J. Fluid Mech. (1984), *vol.* 149, *pp.* 255–273
Printed in Great Britain

The effects of turbulence on the mean flow past two-dimensional rectangular cylinders

By YASUHARU NAKAMURA AND YUJI OHYA
Research Institute for Applied Mechanics, Kyushu University, Kasuga, 816, Japan

(Received 24 January 1984)

There are two main effects of turbulence on the mean flow past rectangular cylinders, just as found earlier for square rods. Small-scale turbulence increases the growth rate of the separated shear layers through increased mixing. Large-scale turbulence weakens regular vortex shedding by reducing spanwise correlation. The consequences of increased mixing and weakened regular vortex shedding depend on the depth-to-height ratio of a rectangular cylinder. In particular, the mean base pressure of a rectangular cylinder can be varied significantly by both the scale and intensity of turbulence.

1. Introduction

It has been shown by past investigations that the time-mean drags of bluff bodies with sharp-edged separation can be strongly influenced by the turbulence of the approaching flow. However, it has also been shown that there is very little or no effect of turbulence scale, despite a significant effect of turbulence intensity. This applies to two-dimensional bluff bodies such as rectangular cylinders, including a square (Bearman 1972; Laneville, Gartshore & Parkinson 1975; Nakamura & Tomonari 1976; Petty 1979; Laneville & Williams 1979), and also a cube, which is one of the most typical three-dimensional bluff bodies (Roberson *et al.* 1972; Bearman 1980). The only exception where there is a significant effect of turbulence scale is for square and circular plates that are placed normal to the flow (Bearman 1971). Such a situation was very difficult to understand, and had long been an enigma related to the effects of turbulence on the mean flow past sharp-edged bluff bodies (Bearman 1978).

In a previous paper (Nakamura & Ohya 1983) we challenged this problem by making measurements on the mean flow past three-dimensional rods of square cross-section with various lengths aligned with the grid-generated turbulent flow where the scale and intensity of turbulence were widely varied. It was found that there are two main effects of turbulence, namely those of small-scale (relative to body size) and large-scale (comparable to body size) turbulence. Small-scale turbulence can increase the growth rate of the separated shear layers of a square rod, while large-scale turbulence can enhance the roll-up of the shear layers. Thus it has become clear that the mean flow past square rods can be influenced significantly by both the scale and intensity of turbulence.

The present paper is a continuation of our work on the three-dimensional square rods, and it is concerned mainly with measurements of the mean static-pressure distributions on the surface and along the wake of a two-dimensional rectangular cylinder that was placed normal to the grid-generated turbulent flow. In the experiment the depth-to-height ratio d/h of a rectangular cylinder was varied from

0.2 to 1.0, where d and h are respectively the depth and height of the rectangular cylinder. Cylinders of various sizes were mounted at a location downstream of a turbulence-producing grid. The ratio L_x/h of turbulence scale to cylinder height ranged from 0.21 to 14 approximately for two different values of the turbulence intensity u'/U of 6% and 10% approximately; here L_x and u' are respectively the integral scale and the r.m.s. value of the longitudinal velocity of turbulence, and U is the mean free-stream speed. The results of the present investigation have shown that the mean flow past rectangular cylinders can be influenced significantly by the approaching turbulence, and it depends strongly on both the scale and intensity of the turbulence.

2. Experimental arrangements

2.1. *Wind tunnel and turbulence-producing grid*

The experiments were conducted in a wind tunnel with a 4 m high by 2 m wide by 6 m long rectangular working section. The tunnel can provide a very uniform smooth flow with a turbulence intensity of about 0.12%. To create a nearly homogeneous isotropic turbulence field, two square-mesh biplanar grids of rectangular-section bars were used. They had $M = 60$ cm, $b = 15$ cm and $M = 13$ cm, $b = 2.5$ cm respectively, where M and b are the mesh and the bar sizes of the grid. These two grids are hereinafter referred to as the large and the small grid respectively. The 6 m long working section was too short for the experiment using the large grid to be made, so the diffuser was modified to extend the length of the working section by 6 m. The characteristics of the grid turbulence relevant to the present measurements are given in table 1. A more detailed description of the grids and the turbulence characteristics is found in Nakamura & Ohya (1983).

2.2. *Models and measurement procedures*

The models used in the present investigation were rectangular plywood cylinders with four different values of the depth-to-height ratio of 0.2, 0.4, 0.6 and 1.0 (square). The height of the rectangular cross-section of the cylinders was varied from 2 to 15 cm. As shown in figure 1, the model was mounted horizontally in the working section, with the front face normal to the flow. In order to avoid any strong interference of the wall boundary layers, the model had square end plates of 120 cm, which were 15 cm away from the sidewalls.

Surface static pressures were measured by using pressure taps of 0.3 mm diameter. Wake static pressures were measured by using a long pressure tube of 2 mm diameter, set along the model centreline, which had four equally spaced holes of 0.3 mm diameter on its circumference. In addition to the pressure measurements, measurements of the u-component velocity in the near wake were made using a hot wire $1h$ downstream and $1h$ below the rear edge of the cylinder, from which power spectra were obtained. Correlations of two u-component velocities along the span were also made using two hot wires $1h$ downstream and $1h$ below the rear edge of the cylinder and separated by a spanwise distance z. The pressure was determined with a calibrated inductance-type pressure transducer, and the mean pressure p is presented in the form of a pressure coefficient $C_p = (p-p_0)/(\frac{1}{2}\rho U^2)$, where ρ and p_0 are respectively the air density and the mean static pressure of the free stream. The values of p_0 and U were determined with a Pitot-static tube placed at the model position in the empty working section.

The main purpose of this investigation was to examine the effect of turbulence scale.

	x/M	u'/U (%)	L_x (cm)
Large grid	10	10.0	19.7
	18	6.1	28.0
Small grid	7	10.8	3.2
	14	6.1	4.4

TABLE 1

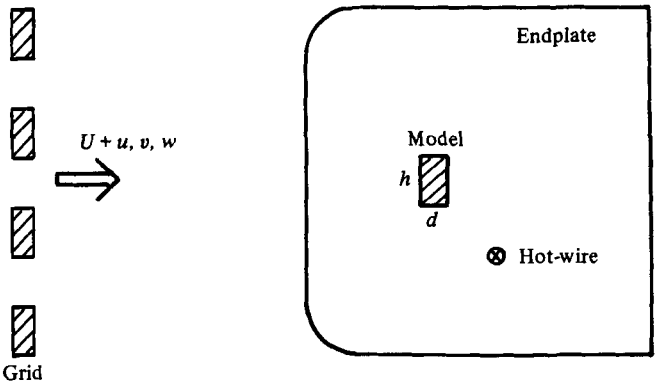

FIGURE 1. Rectangular-cylinder model mounted downstream of a turbulence-producing grid.

This was done by working with different sizes of cylinders using two grids with different mesh sizes. The measurements corresponded to two different values of turbulence intensity of approximately 6% and 10% (see table 1). All the measurements were made at a constant flow speed of 10 m s^{-1}, except for some supplementary ones. Correspondingly, the values of the Reynolds number, based on h, ranged from 1.4×10^4 to 10^5 approximately.

3. Experimental results

The measurements were concerned with rectangular cylinders with different sizes, mounted in the closed working section, and exposed to flow of a constant speed. There are many factors, apart from turbulence, that can affect the mean flow past a rectangular cylinder. These include, among others, the Reynolds number, the tunnel blockage, and the finite aspect ratio of a rectangular cylinder.

3.1. *Reynolds-number effect*

Figure 2 shows the variations of the base-pressure coefficients for smooth flow with the Reynolds number for rectangular cylinders with four different depth-to-height ratios. The measurements were made using cylinders with a height of 10 cm. As can be seen, the base-pressure coefficient for $d/h = 0.2$ is sensibly constant over the tested range, while those for the rest increase gradually as the Reynolds number is lowered below approximately 3.3×10^4. A similar Reynolds-number effect was also observed by Bearman & Trueman (1972) and Courchesne & Laneville (1979).

If there is no Reynolds-number effect for smooth flow, it may well be assumed that there is also no such effect for turbulent flow. On the other hand, if there is a Reynolds-number effect for smooth flow, the results for turbulent flow may also be

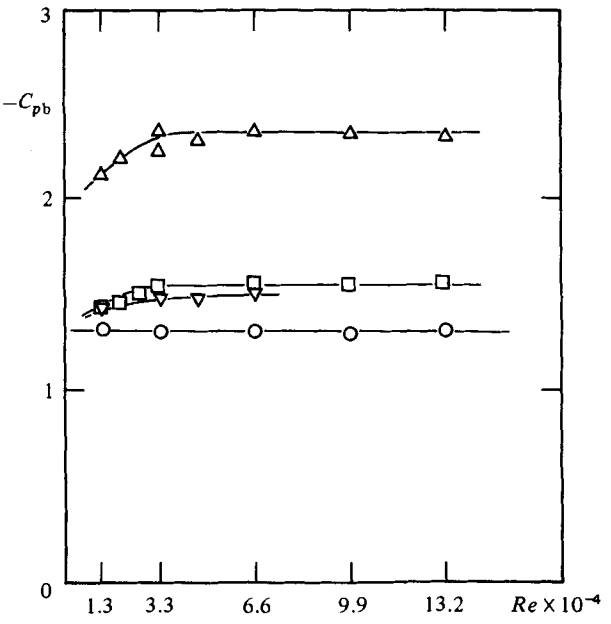

FIGURE 2. Reynolds-number dependence of the base-pressure coefficients for smooth flow: ○, $d/h = 0.2$; ▽, 0.4; △, 0.6; □, 1.0.

Reynolds-number dependent. The values of the Reynolds number corresponding to the 2 and 3 cm cylinders were 1.4×10^4 and 2.1×10^4, and fell within the above-mentioned sensitive range. However, it was difficult to raise the Reynolds number much further by increasing the flow speed, because it would cause a possible failure of the wooden grids due to high drag forces.

3.2. *Blockage correction*

The results of measurement of the base-pressure coefficient for smooth flow using rectangular cylinders with various sizes are shown in figure 3 for the four different depth-to-height ratios. It is seen that base pressures decrease proportionally with the blockage ratio h/H over the tested range, where H is the tunnel height. This allows the uncorrected base-pressure coefficient C_{pb} to be expressed using the corrected one C_{pbc} as

$$C_{pb} = C_{pbc}\left(1 + \xi \frac{h}{H}\right), \tag{1}$$

where ξ is the correction factor. Obviously, both the corrected base-pressure coefficient and the correction factor are dependent on the depth-to-height ratio of a cylinder. Figure 4 shows the correction factor plotted against the corrected base-pressure coefficient with the depth-to-height ratio as a parameter. In the figure supplementary results for $d/h = 0.5$, 0.7 and 1.67 are also added. As can be seen, the blockage effect is largest near the critical cylinder where the base-pressure coefficient shows an abrupt minimum (see §4). This is in contrast with the conclusion of Courchesne & Laneville (1979), who reported that it was smallest near the critical cylinder. The reason for this difference is not clear.

No satisfactory correction method has been proposed to account for the blockage effects on the flow past two-dimensional bluff bodies. Maskell (1965), among

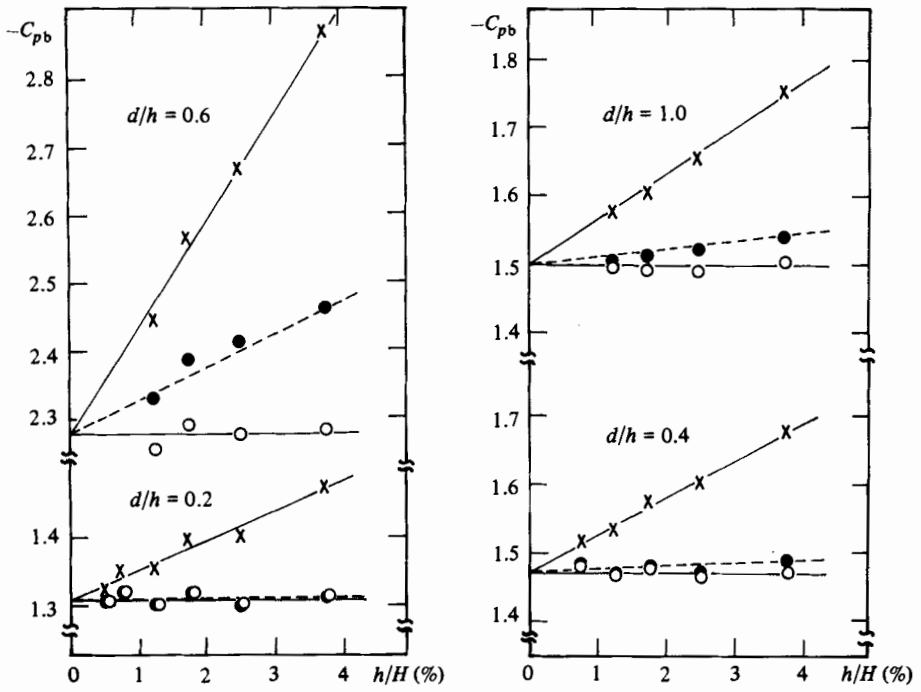

FIGURE 3. Blockage effect for the base-pressure coefficients for smooth flow: ×, experiment; ○, equation (1); ●, Maskell.

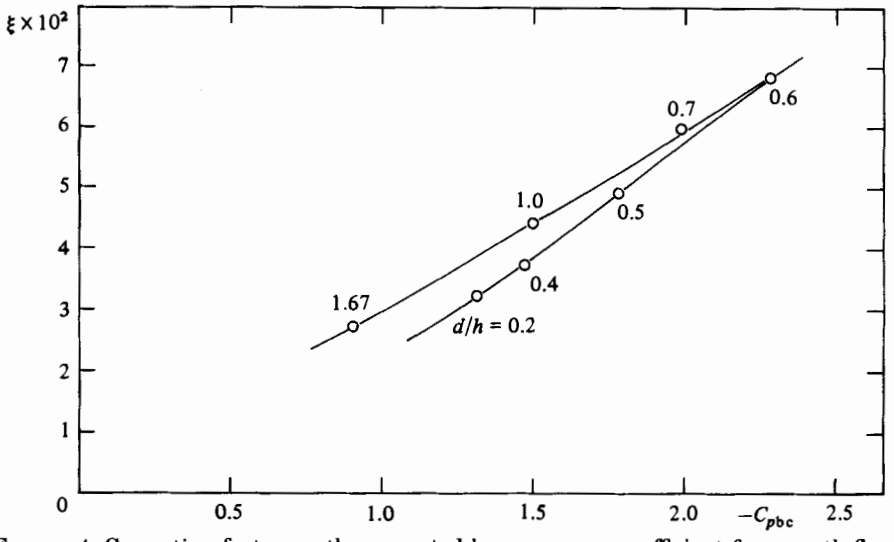

FIGURE 4. Correction factor *vs.* the corrected base-pressure coefficient for smooth flow. Depth-to-height ratio is plotted as a parameter.

others, gave a correction method for bluff bodies by using a simple free-streamline representation of the wake and considering the momentum balance in the external flow. The method was shown to give good results for flat plates normal to the flow up to about 10% blockage ratio, but for other rectangular cylinders such as a square one the results were found to be rather unsatisfactory (Petty 1979; Courchesne & Laneville 1979; see also figure 3 of this paper).

In the present investigation we have adopted a more empirical correction method applying to turbulent flow which is based on the results of figure 4. We assume, as Maskell did, that the pressure distributions for the confined flow past rectangular cylinders are similar, so the only effect of blockage is to produce an apparent increase in the free-stream speed. For turbulent flow, both the base-pressure coefficient and the correction factor are dependent not only on the depth-to-height ratio but also on the free-stream turbulence. Without any rigorous arguments, our method of blockage correction assumes that the curve of figure 4 showing the relation between the correction factor and the corrected base-pressure coefficient for smooth flow is also applicable to turbulent flow. Namely, once the uncorrected base-pressure coefficient for turbulent flow is known experimentally, the corrected one is obtained by iteration with the combined use of (1) and the curve of figure 4. This gives rise to the corrected value of the free-stream speed for turbulent flow. For the sake of convenience, the notation C_{pb} is hereinafter used for the corrected base-pressure coefficient.

3.3. *Spanwise pressure distributions*

Figures 5(a, b) present some examples of the spanwise pressure distributions for smooth and turbulent flows respectively. It is seen that pressure along the span is reasonably uniform for both smooth and turbulent flows.

3.4. *Base-pressure coefficients, longitudinal pressure distributions and power spectra of velocity fluctuations in the near wake*

Figure 6(a) shows the base-pressure coefficients of rectangular cylinders with $d/h = 0.2$ and 0.4 for turbulent flow, plotted against the ratio of turbulence scale to cylinder height L_x/h, while figure 6(b) shows those of rectangular cylinders with $d/h = 0.6$ and 1.0. The corresponding values for smooth flow are also included in the same figures. The results in figures 6(a, b) using two different grids show satisfactory collapses. No significant effects of the Reynolds number on the base-pressure coefficients were observed for most tested cases. The only results that showed Reynolds-number dependence were those for the 2 cm cylinders using the large grid (highest L_x/h tested) for the three depth-to-height ratios other than $d/h = 0.2$. For this reason these data are not shown in figures 6(a, b). Satisfactory collapses of the experimental results also confirm the validity of the method of blockage correction adopted in the present investigation.

What is most interesting in figures 6(a, b) is the presence of the significant effects of turbulence scale. Just as found earlier for square rods (Nakamura & Ohya 1983), there are two main effects of turbulence, namely those of small- and large-scale turbulence. Here small-scale turbulence specifically refers to the case in which the size of the energy-containing eddies is comparable to the thickness of the separated shear layer, while large-scale turbulence refers to the case in which the size of the energy-containing eddies is comparable to that of the whole near wake.

Small-scale turbulence reduces the base pressure of a short rectangular cylinder ($d/h = 0.4$), while it increases that of a long rectangular cylinder ($d/h = 0.6$ and 1.0). In particular, small-scale turbulence does not alter the base pressure of a very short rectangular cylinder ($d/h = 0.2$), while the base pressure of the square cylinder does not vary with L_x/h over this range, although it is considerably higher than the smooth-flow value. These have been the main sources of the enigma related to turbulence effects on bluff-body mean flow, as mentioned in §1.

The effect of large-scale turbulence, on the other hand, is found to increase the base

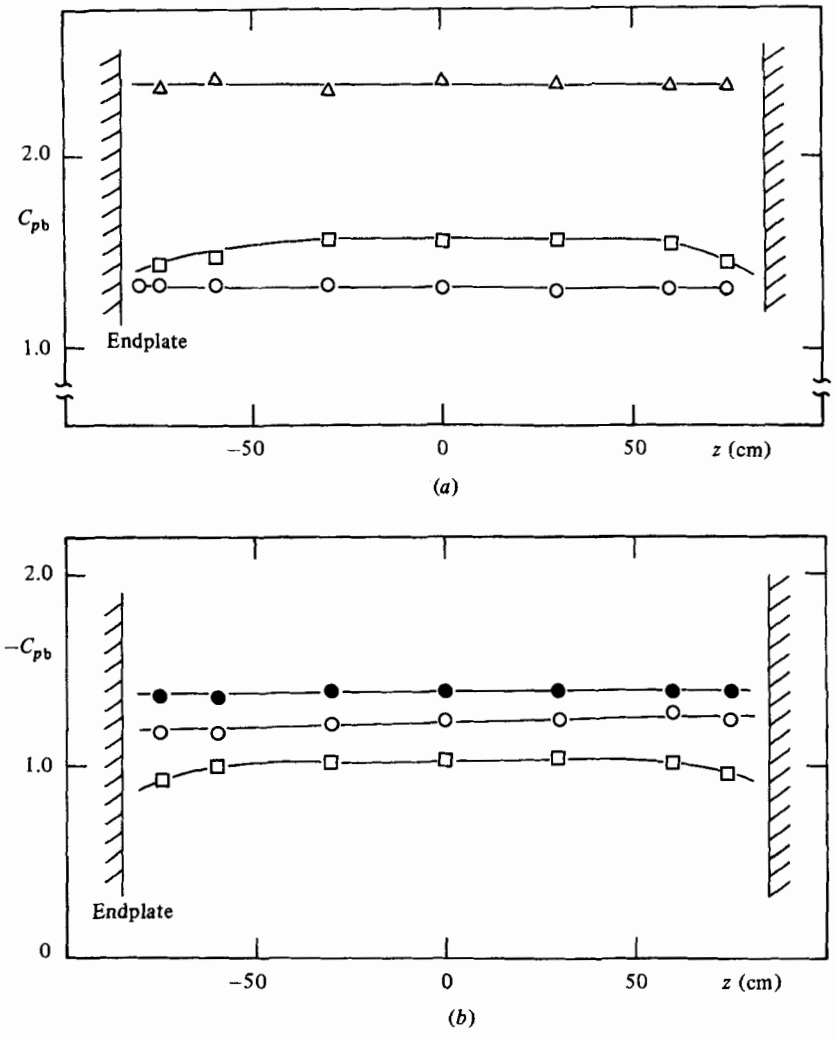

FIGURE 5. Spanwise variations of the base-pressure coefficients. (*a*) Smooth flow: ○, $d/h = 0.2$; △, 0.6; □, 1.0. (*b*) Turbulent flow: ●, $d/h = 0.2$, $u'/U = 10.8\%$, $L_x/h = 0.32$; ○, 0.2, 10.0%, 1.97; □, 1.0, 10.8%, 0.32.

pressure of the rectangular cylinders tested, except for the square one. Base pressure increases with increase in L_x/h, reaching a maximum at about $L_x/h = 3.0$, and then decreases gradually back to the smooth-flow value. Accordingly, the effect of large-scale turbulence is most marked at about $L_x/h = 3.0$.

Figures 7(*a–d*) show the longitudinal pressure distributions on the side face and along the wake-centreline of rectangular cylinders with $d/h = 0.2$, 0.4, 0.6 and 1.0 respectively for smooth flow and for small- and large-scale turbulence. Here again, the effects of small- and large-scale turbulence are evident. The variation of the minimum pressure in the near wake closely follows the trend observed for the base-pressure variations. In particular, small-scale turbulence considerably reduces the value of the minimum pressure of a rectangular cylinder with $d/h = 0.4$. A similar trend is seen for a rectangular cylinder with $d/h = 0.2$, although it is less obvious. Also, large-scale turbulence increases the value of the minimum pressure for the rectangular cylinders tested, except for the square one.

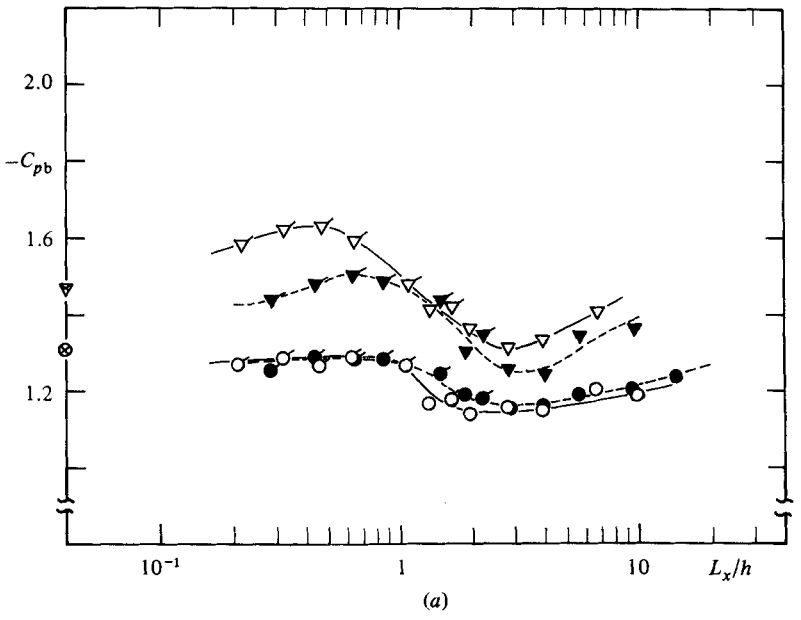

(*a*)

FIGURE 6(*a*). For caption see facing page.

The minimum pressure in the wake is a result of the formation of regular vortex shedding (§4). Figures 8(*a–c*) compare the power spectra of the u-component velocity measured at a location $1h$ downstream and $1h$ below the rear edge of a rectangular cylinder with $d/h = 0.4$ for smooth flow and for small- and large-scale turbulence. Figures 9(*a–c*) also compare those of a rectangular cylinder with $d/h = 0.6$. If it is assumed that the spectral peak of the fluctuating velocity indicates the strength of regular vortex shedding, one may infer the following. Small-scale turbulence strengthens regular vortex shedding behind a short rectangular cylinder ($d/h = 0.4$), while it weakens regular vortex shedding behind a long rectangular cylinder ($d/h = 0.6$). On the other hand, large-scale turbulence weakens regular vortex shedding behind a rectangular cylinder, whether short or long. It should be added that the frequency of regular vortex shedding was not appreciably influenced by small- and large-scale turbulence. The behaviour of regular vortex shedding thus inferred is compatible with the observations on base pressure and the minimum pressure in the near wake.

3.5. *Spanwise correlation of regular vortex shedding*

Measurements were made of the spanwise correlation of the u-component velocities for smooth flow and for small- and large-scale turbulence. As before, the hot wires were placed $1h$ downstream and $1h$ below the rear edge of a rectangular cylinder. Figure 10(*a*) shows the measurement results for the coherency at the vortex-shedding frequency for a rectangular cylinder with $d/h = 0.2$. Here the coherency $\gamma^2(f)$ at a frequency f for the spanwise locations z_1 and z_2 is given by

$$\gamma^2(f) = \frac{|P_{z_1 z_2}(f)|^2}{P_{z_1 z_1}(f)\, P_{z_2 z_2}(f)}, \tag{2}$$

where $P_{z_1 z_2}(f)$ is the cross-spectrum, and $P_{z_1 z_1}(f)$ and $P_{z_2 z_2}(f)$ are the power spectra. It is interesting that the coherency for small-scale turbulence is almost identical with

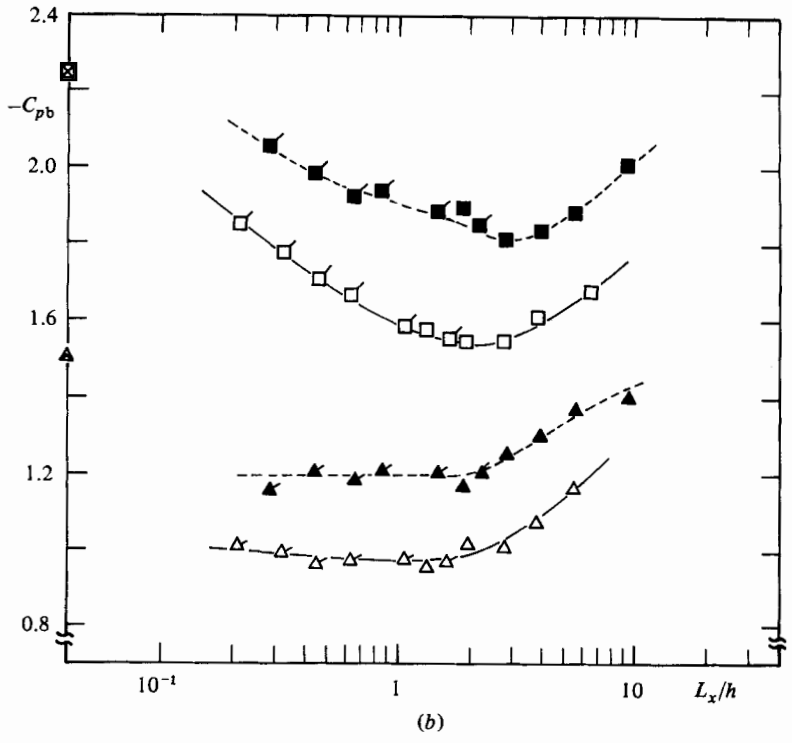

FIGURE 6. Base-pressure coefficients *vs.* the ratio of turbulence scale to cylinder height. (*a*) $d/h = 0.2$ and 0.4:

		Small grid		Large grid	
d/h	Smooth flow	6.1% (u'/U)	10.8%	6.1%	10.0%
0.2	⊗	●	○	●	○
0.4	▽	▼	▽	▼	▽

(*b*) $d/h = 0.6$ and 1.0:

		Small grid		Large grid	
d/h	Smooth flow	6.1% (u'/U)	10.8%	6.1%	10.0%
0.6	⊠	■	□	■	□
1.0	△	▲	△	▲	△

that for smooth flow, while that for large-scale turbulence is considerably lower. It is worth mentioning that the results for the correlation of unfiltered signals may be misleading on this point. As is seen in figure 10(*b*), the unfiltered correlation for small-scale turbulence is lower than that for large-scale turbulence at small separations, although it becomes higher at large separations. The results for the coherency and correlation for rectangular cylinders with $d/h = 0.4$ and 0.6 are shown in figures 11(*a*, *b*) and 12(*a*, *b*).

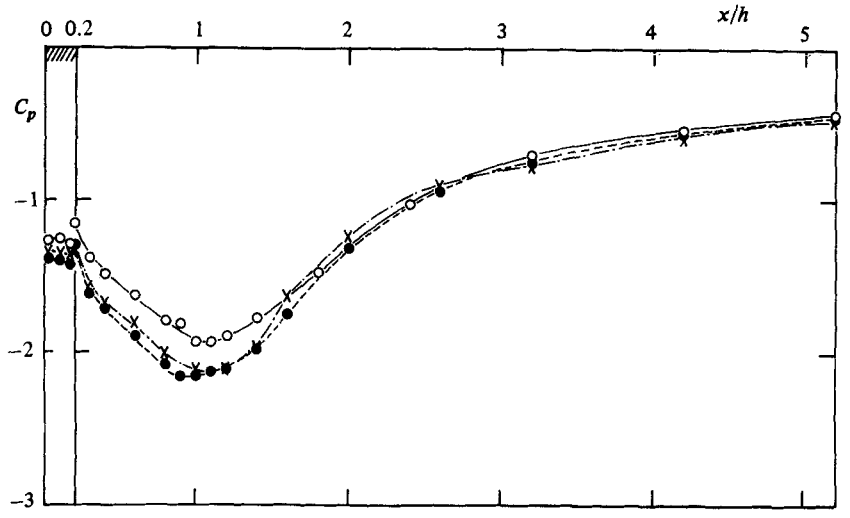

(a)

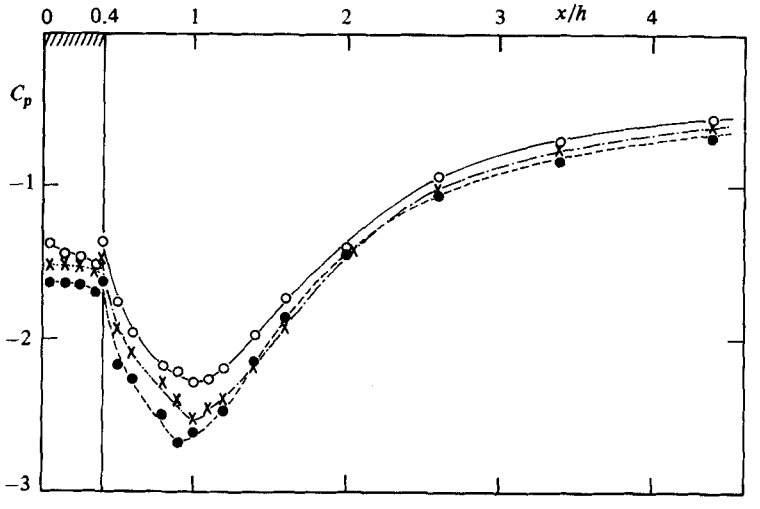

(b)

FIGURE 7(a, b). For caption see facing page.

4. The shear-layer–edge direct interaction

In order to assess turbulence effects correctly, it is convenient to consider the two main aspects of bluff-body flow separately; namely, the shear-layer growth and vortex formation in a section on the one hand, and the spanwise correlation of vortex formation on the other.

On a flat plate normal to the flow, the two separated shear layers are basically unstable, and roll up to form discrete vortices. During formation, the vortices, and the shear layers to a lesser extent, draw in fluids from the base region, and this leads to low base pressure (Bearman 1972).

The work by Nakaguchi, Hashimoto & Muto (1968) on rectangular cylinders

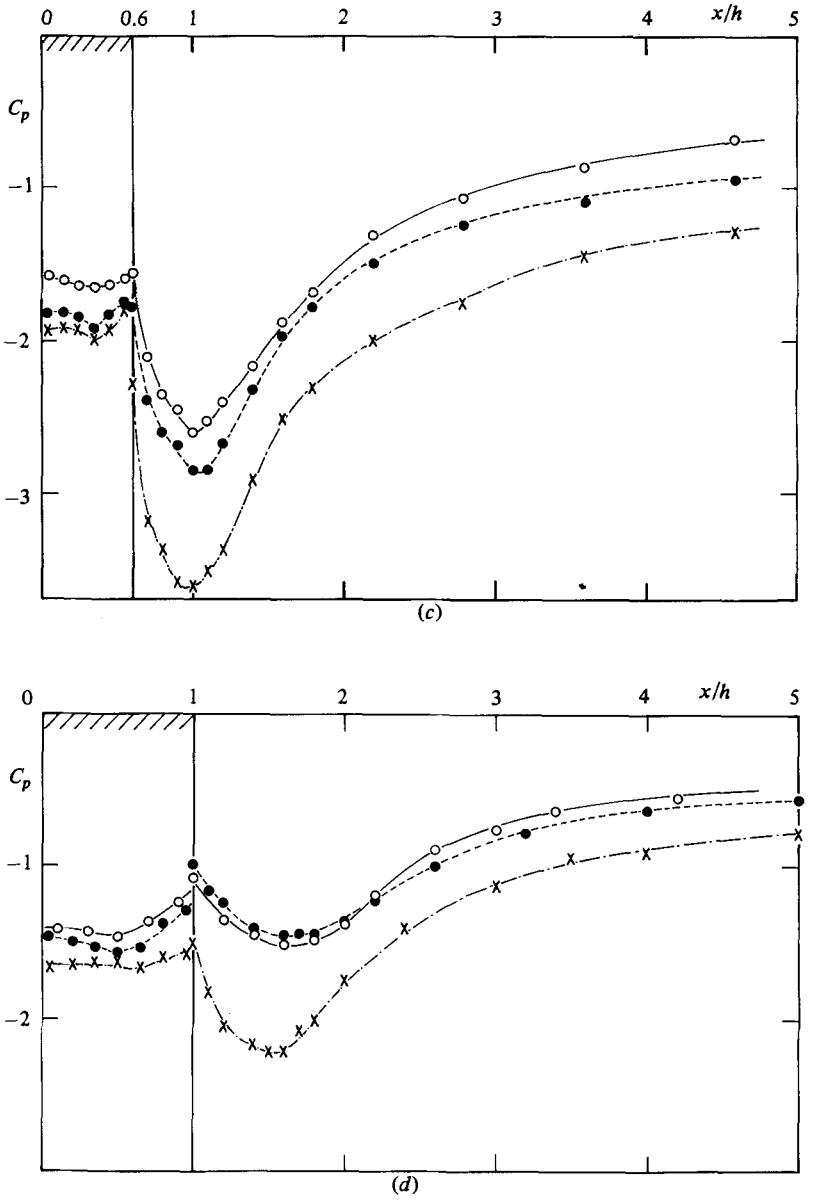

FIGURE 7. Pressure distributions on the side face and along the wake centreline for smooth flow and for small- and large-scale turbulence. (*a*) $d/h = 0.2$; (*b*) 0.4; (*c*) 0.6; (*d*) 1.0. ×, smooth flow; ●, small-scale turbulence, $u'/U = 10.8\,\%$, $L_x/h = 0.32$; ○, large-scale turbulence, $u'/U = 10.0\,\%$, $L_x/h = 1.97$, except for $d/h = 1.0$, where $L_x/h = 3.94$ for large-scale turbulence.

showed that, as the cylinder depth increases from zero, the base pressure decreases rapidly to a critical minimum at a depth just beyond 0.6 times the height. The decrease in base pressure for cylinders shorter than the critical is associated with an increased curvature of the shear layer in roll-up (Nakaguchi *et al.* 1968). The increase in base pressure for cylinders longer than the critical is associated with the direct interaction of the downstream edge with the shear layer by which vortex formation is delayed further downstream (Bearman & Trueman 1972). It should be added that

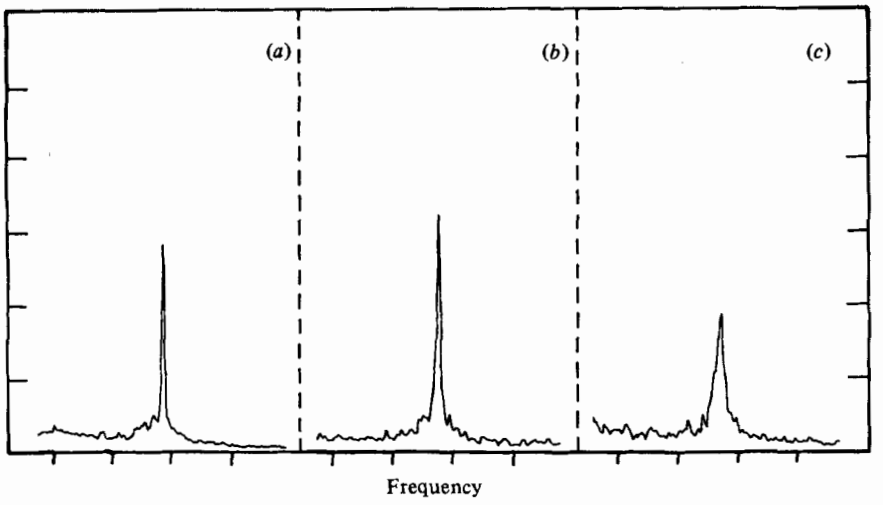

FIGURE 8. Spectra of the u-component velocity for $d/h = 0.4$: (a) smooth flow; (b) small-scale turbulence; (c) large-scale turbulence. Flow conditions are the same as in figure 7(b).

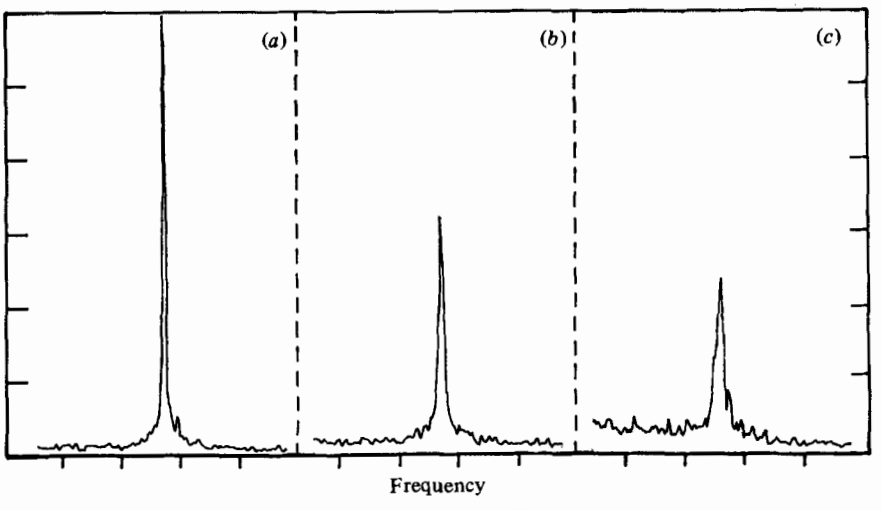

FIGURE 9. Spectra of the u-component velocity for $d/h = 0.6$: (a) smooth flow; (b) small-scale turbulence; (c) large-scale turbulence. Flow conditions are the same as in figure 7(c).

the shear-layer–edge direct interaction also yields a side-face pressure distribution of reattachment type, that is, low pressure followed by high pressure of some level, which is similar to that of a reattaching flow (Nakamura & Tomonari 1981).

In the case where the approaching flow is turbulent, the combined effects of turbulence and depth-to-height ratio should appear.

5. The effects of small-scale turbulence

It has been widely recognized that small-scale turbulence can accelerate the growth of the separated shear layer through increased mixing, thus leading to enhanced entrainment of fluids from the near wake. In the present measurements, it is found that small-scale turbulence does not significantly reduce the spanwise correlation of

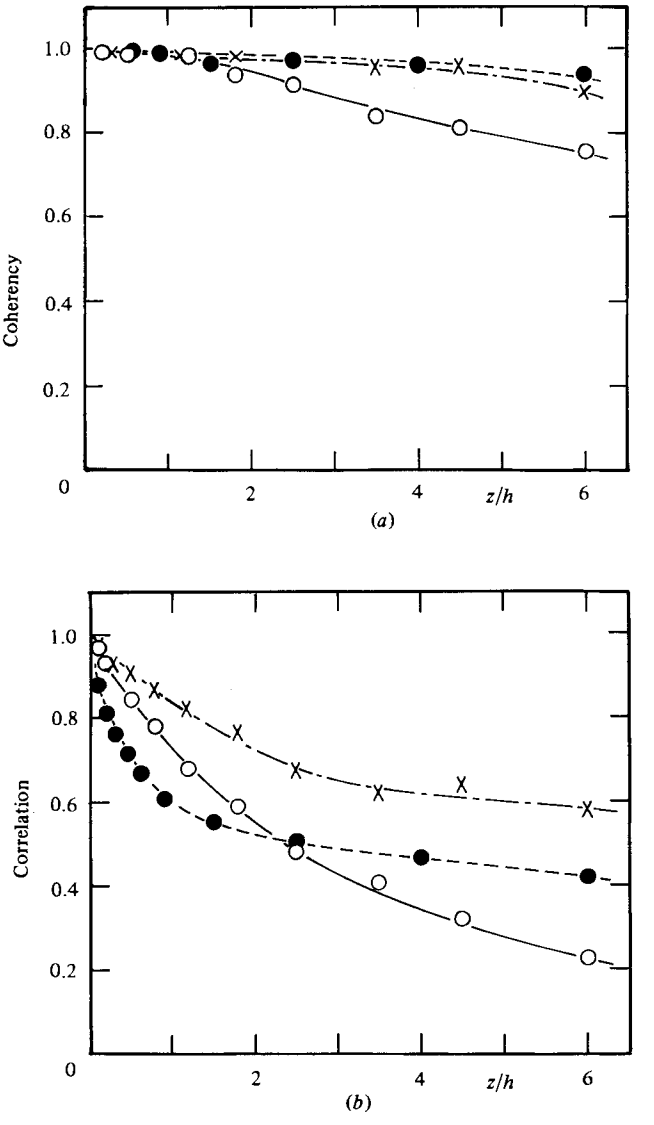

FIGURE 10. Coherency and correlation of the u-component velocities for $d/h = 0.2$ for smooth flow and for small- and large-scale turbulence: (*a*) coherency at the vortex frequency; (*b*) correlation of the unfiltered signals. For legend see figure 7 (*a*).

vortex shedding for a rectangular cylinder (figures 10–12). Accordingly, the main effect of small-scale turbulence is to promote the shear-layer–edge direct interaction, or, in short, to lower the value of the critical depth for a rectangular cylinder.

Figure 13 shows the variation of the base-pressure coefficient with the depth-to-height ratio for smooth flow and for small-scale turbulence with $L_x/h = 0.63$ and $u'/U = 6.1\,\%$ approximately. The trend shown in figure 13 is in agreement with earlier measurements (Nakamura & Tomonari 1976; Courchesne & Laneville 1982), and indicates appreciable reduction in critical depth due to small-scale turbulence. It can be said that small-scale turbulence yields lower base pressure (and stronger vortex shedding) for a short rectangular cylinder, and higher base pressure (and weaker vortex shedding) for a long rectangular cylinder.

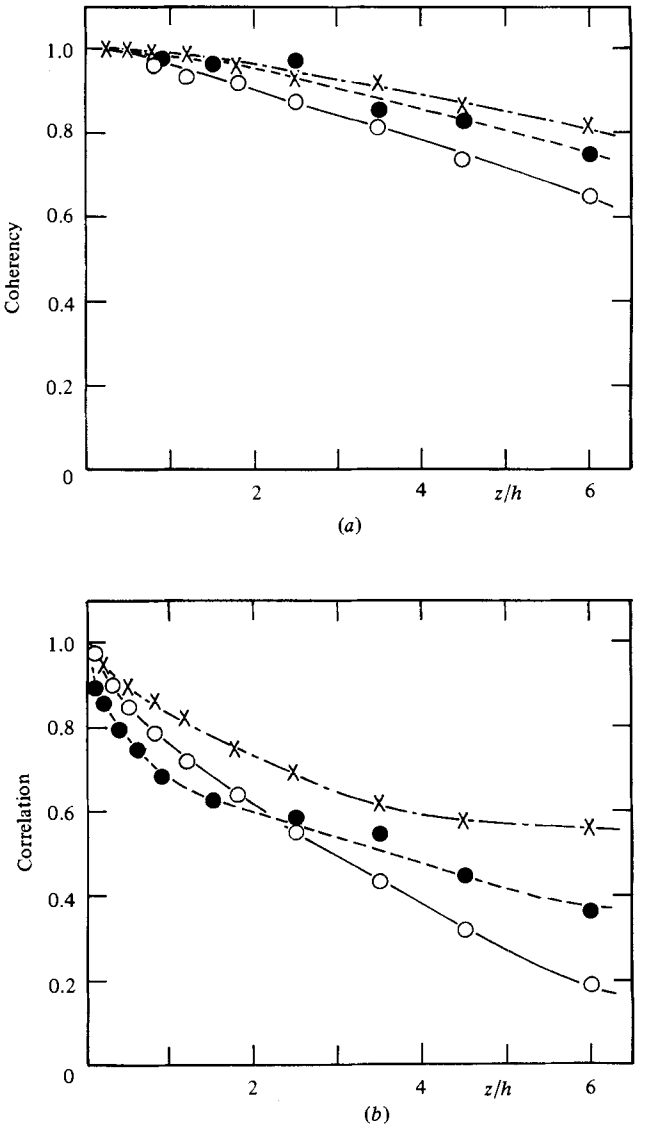

FIGURE 11. Coherency and correlation of the u-component velocities for $d/h = 0.4$ for smooth flow and for small- and large-scale turbulence: (a) coherency at the vortex frequency; (b) correlation of the unfiltered signals. For legend see figure 7 (b).

6. The interaction of large-scale turbulence with regular vortex shedding

Obviously, the effects of small-scale turbulence should become weakened as turbulence scale is increased further. However, large-scale turbulence can control the near wake differently. As is shown in figures 10–12, large-scale turbulence weakens regular vortex shedding by reducing its spanwise correlation. The influence must be most significant for the turbulence scale that is roughly as large as the size of the near wake. This characterizes the interaction of large-scale turbulence with regular vortex shedding.

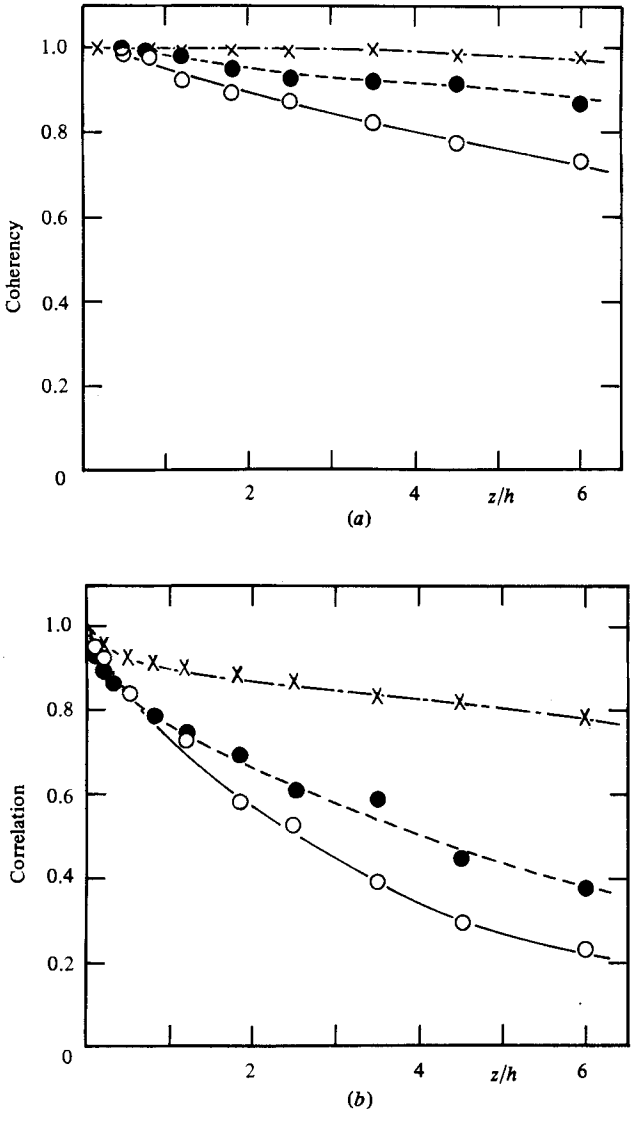

FIGURE 12. Coherency and correlation of the u-component velocities for $d/h = 0.6$ for smooth flow and for small- and large-scale turbulence: (*a*) coherency at the vortex frequency; (*b*) correlation of the unfiltered signals. For legend see figure 7(*c*).

7. Turbulence effects on two- and three-dimensional sharp-edged bluff-body mean flow

It may be instructive to summarize the main effects of turbulence scale on the mean flows past two- and three-dimensional sharp-edged bluff bodies. For small-scale turbulence, there is basically no difference between the effects on the two-dimensional bluff-body mean flow and those on the three-dimensional bluff-body mean flow. The underlying fluid-mechanical phenomenon that is common to these two is the increased entrainment of fluids from the near wake due to turbulence. For large-scale turbulence there is an apparent difference between the two. Namely, large-scale

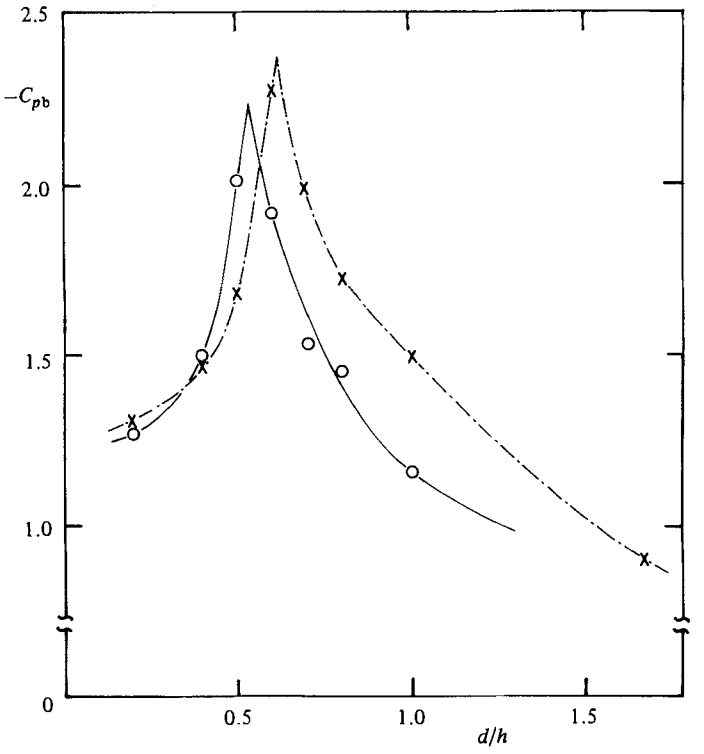

FIGURE 13. Base-pressure coefficients *vs.* depth-to-height ratio: ×, smooth flow; ○, small-scale turbulence, $u'/U = 6.1\,\%$, $L_x/h = 0.63$.

turbulence increases the base pressure of a two-dimensional flat plate, while it reduces that of a three-dimensional square plate. In other words, large-scale turbulence impedes regular vortex shedding of the former, while it enhances the roll-up of the latter. However, it should be remarked that both of the effects are attributable to the three-dimensional character of turbulence.

8. Some further remarks

8.1. *The location of the minimum pressure in the near wake*

As mentioned in §4, Bearman & Trueman (1972) assumed that the shear-layer–edge direct interaction causes vortex formation to be delayed further downstream to produce higher base pressure. However, the present experimental results for turbulent flow do not lend support to this idea. As figures 7 (*c*, *d*) indicate, the minimum pressure in the near wake is considerably increased in small- and large-scale turbulence, but with no significant downstream movement of its location. It appears that the concept of delayed vortex formation needs some modification. On the other hand, the shear-layer–edge direct interaction produces side-face pressure distributions of reattachment type in both smooth and turbulent flows. This can be seen also in figures 7 (*c*, *d*).

8.2. *The results for the square cylinder*

The square cylinder is the one whose experimental results still remain beyond understanding. The mechanism by which base pressure does not vary over a range

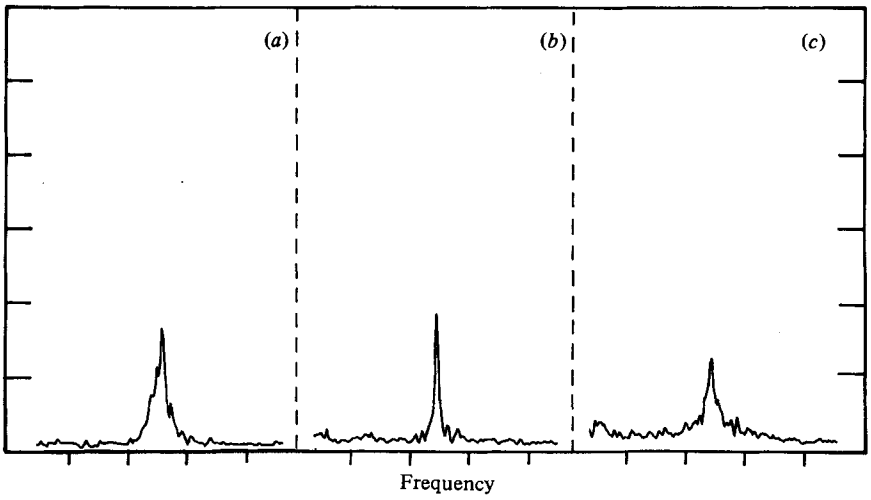

FIGURE 14. Spectra of the u-component velocity for $d/h = 1.0$: (a) smooth flow; (b) small-scale turbulence; (c) large-scale turbulence. Flow conditions are the same as in figure 7(d), except for large-scale turbulence, where $L_x/h = 1.97$.

of small-scale turbulence remains unclear. It is expected that, for cylinders longer than the square one, the range of turbulence scale in which base pressure is constant may be extended. Hillier & Cherry (1981) found no scale effects up to $L_x/h = 1.95$ on the separating-and-reattaching flow formed by a long plate with a blunt face. Similar base-pressure variations were found for a cube and a square rod with a length-to-size ratio of 2.0 (Nakamura & Ohya 1983).

It also remains unclear how large-scale turbulence affects regular vortex shedding behind the square cylinder. We have found that there is some difference in the forms of the power spectrum, the coherency and the correlation of fluctuating velocities between the square cylinder and the other shorter ones. The results for the square cylinder are shown in figures 14(a–c) and 15(a, b), and await further study.

8.3. *The effect of the Reynolds number in turbulent flow*

At low Reynolds numbers the point of transition from laminar to turbulent can move considerably along the separated shear layer with the Reynolds number. The interaction between the shear layer and the afterbody of a bluff body may then be Reynolds-number dependent. Tomonari found, in his study of transverse galloping of the square cylinder at low Reynolds numbers (Tomonari 1982), that, as the Reynolds number was increased from 10^3 to 10^4 approximately, the transition point moved forward beyond the rear edge of the cylinder, thereby causing a drastic change in the lateral aerodynamic force characteristics. In the present measurements of the base pressures of rectangular cylinders in turbulent flow, no significant effects of the Reynolds number were observed over a range of small-scale turbulence at low Reynolds numbers where significant effects were present in smooth flow. Such effects were observed only at high values of the turbulence-scale ratio, say $L_x/h = 10$–14. This may be understandable if we remember that it is small-scale turbulence that can accelerate the forward movement of the transition point.

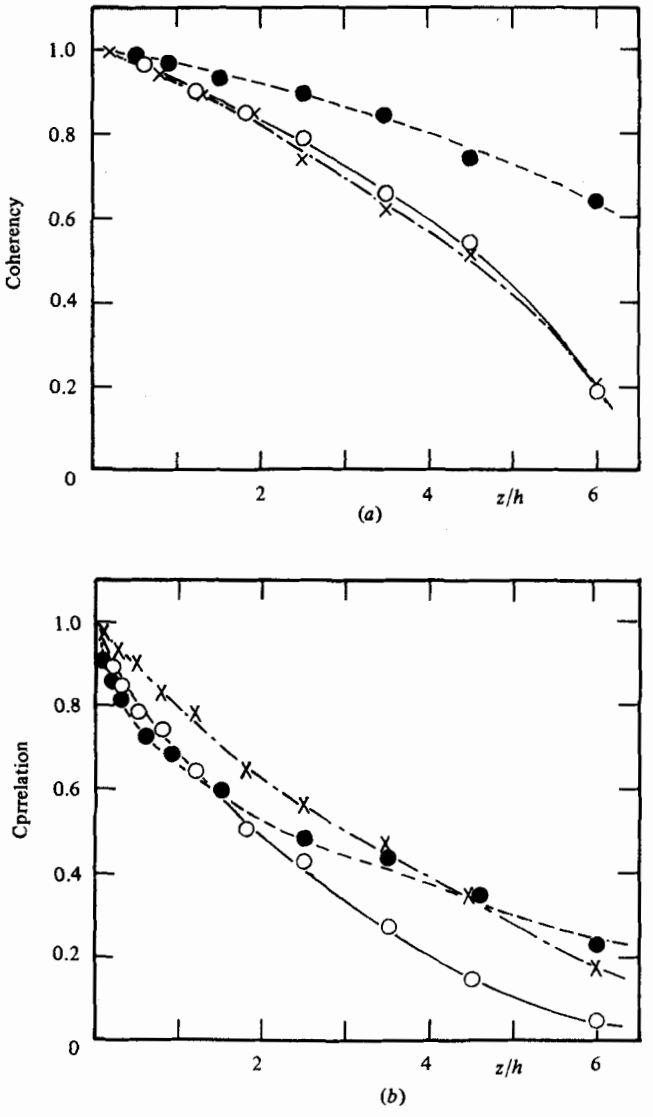

FIGURE 15. Coherency and correlation of the u-component velocities for $d/h = 1.0$: (a) coherency at the vortex frequency; (b) correlation of the unfiltered signals. For legend see figure 7 (d), except for large-scale turbulence, where $L_x/h = 1.97$.

9. Conclusions

There are two main effects of turbulence on the mean flow past rectangular cylinders, just as found earlier for square rods. Small-scale turbulence can accelerate the growth rate of the separated shear layers through enhanced entrainment of fluids from the near wake. For short cylinders it leads to lower base pressure and stronger vortex shedding with increased shear-layer curvature, while for long cylinders it leads to higher base pressure and weaker vortex shedding through the promotion of the shear-layer–edge direct interaction.

On the other hand, large-scale turbulence weakens vortex shedding behind rectangular cylinders, whether short or long, by reducing spanwise correlation, thus

increasing base pressure. The effect is most marked at a ratio of turbulence scale to cylinder height of about 3. The effects of turbulence on the mean flow past the square and longer rectangular cylinders need further study.

Technical assistance from Mr K. Watanabe and Mr A. Nagano is gratefully acknowledged. This work was supported in part by a grant from the Ministry of Education, Science and Culture of Japan.

REFERENCES

BEARMAN, P. W. 1971 An investigation of the forces on flat plates normal to a turbulent flow. *J. Fluid Mech.* **46**, 177–198.

BEARMAN, P. W. 1972 Some recent measurements of the flow around bluff bodies in smooth and turbulent streams. In *Proc. Symp. External Flows, University of Bristol*, pp. B1–B15.

BEARMAN, P. W. 1978 Turbulence effects on bluff body mean flow. In *Proc. 3rd US Natl Conf. Wind Engineering Research, University of Florida*, (ed. B. M. Leadon) pp. 265–272.

BEARMAN, P. W. 1980 Review – Bluff body flows applicable to vehicle aerodynamics. *Trans ASME* I: *J. Fluids Engng* **102**, 265–274

BEARMAN, P. W. & TRUEMAN, D. M. 1972 An investigation of the flow around rectangular cylinders. *Aero. Q.* **23**, 229–237.

COURCHESNE, J. & LANEVILLE, A. 1979 A comparison of correction methods used on the evaluation of drag coefficient measurements for two-dimensional rectangular cylinders. *Trans ASME* I: *J. Fluids Engng* **101**, 506–510.

COURCHESNE, J. & LANEVILLE, A. 1982 An experimental evaluation of drag coefficient for rectangular cylinders exposed to grid-turbulence. *Trans ASME* I: *J. Fluids Engng* **104**, 523–528.

HILLIER, R. & CHERRY, N. J. 1981 The effects of stream turbulence on separation bubbles. *J. Wind Engng Indust. Aerodyn.* **8**, 49–58.

LANEVILLE, A., GARTSHORE, I. S. & PARKINSON, G. V. 1975 An explanation of some effects of turbulence on bluff bodies. In *Proc. 4th Intl Conf. Wind Effects on Buildings and Structures* (ed. K. J. Eaton), pp. 333–341. Cambridge University Press.

LANEVILLE, A. & WILLIAMS, C. D. 1979 The effect of intensity and large scale turbulence on the mean pressure and drag coefficients of 2D rectangular cylinders. In *Wind Engineering* (ed. J. E. Cermak), vol. 1, pp. 397–404. Pergamon.

MASKELL, E. C. 1965 A theory of the blockage effects on bluff bodies and stalled wings in a closed wind tunnel. *Aero. Res. Counc. R & M* 3400.

NAKAGUCHI, H., HASHIMOTO, K. & MUTO, S. 1968 An experimental study on aerodynamic drag of rectangular cylinders (in Japanese). *J. Japan Soc. Aero. Space Sci.* **16**, 1–5.

NAKAMURA, Y. & OHYA, Y. 1983 The effects of turbulence on the mean flow past square rods. *J. Fluid Mech.* **137**, 333–347.

NAKAMURA, Y. & TOMONARI, Y. 1976 The effects of turbulence on the drags of rectangular prisms. *Trans. Japan Soc. Aero. Space Sci.* **19**, 81–86.

NAKAMURA, Y. & TOMONARI, Y. 1981 The aerodynamic characteristics of D-section prisms in a smooth and in a turbulent flow. *Aero. Q.* **32**, 153–168.

PETTY, D. G. 1979 The effect of turbulence intensity and scale on the flow past square prisms. *J. Indust. Aerodyn.* **4**, 247–252.

ROBERSON, J. A., LIN, C. Y., RUTHERFORD, G. S. & STINE, M. D. 1972 Turbulence effects on drag of sharp-edged bodies. *J. Hydraul. Div. ASCE* **98** (HY7), 1187–1203.

TOMONARI, Y. 1982 Aeroelastic galloping of square cylinders at low Reynolds numbers (in Japanese). *Bull. Nippon Bunri Univ.* **11**, no. 1, 161–167.